Molecular Pharmacology Fast Forward. Published on August 11, 2022 as DOI: 10.1124/molpharm.122.000545
This article has not been copyedited and formatted. The final version may differ from this version.

Inhibition of the aromatase enzyme by exemestane cysteine conjugates

Irina Teslenko, Christy J.W. Watson, Gang Chen, Philip Lazarus

Department of Pharmaceutical Sciences, College of Pharmacy and Pharmaceutical Sciences, Washington State University, Spokane, WA 99202

Correspondence to Philip Lazarus, PhD Department of Pharmaceutical Sciences, College of Pharmacy and Pharmaceutical Sciences, Washington State University, 412 E. Spokane Falls Blvd., Spokane, WA 99202-2131; Email: phil.lazarus@wsu.edu

Molecular Pharmacology Fast Forward. Published on August 11, 2022 as DOI: 10.1124/molpharm.122.000545
This article has not been copyedited and formatted. The final version may differ from this version.

Running Title: Anti-aromatase activity of exemestane phase II metabolites

Corresponding author: Philip Lazarus, Department of Pharmaceutical Sciences, College of Pharmacy and Pharmaceutical Sciences, Washington State University, 412 E. Spokane Falls Blvd, Spokane, WA 99202. E-mail: phil.lazarus@wsu.edu

Number of text pages:

Number of tables: 2

Number of figures: 4

Number of supplemental figures: 0

Number of references: 52

Number of words:

Abstract: 243

Introduction: 703

Discussion: 1570

Abbreviations: glutathione-S-transferase, GST; exemestane, EXE; 17β-dihydroexemestane, 17β-DHE; 17β -hydroxy-EXE-17-O-b-D-glucuronide, 17β-DHE-

Molecular Pharmacology Fast Forward. Published on August 11, 2022 as DOI: 10.1124/molpharm.122.000545
This article has not been copyedited and formatted. The final version may differ from this version.

Gluc; selective estrogen modulators, SERM; aromatase inhibitor, AI; tamoxifen, TAM; cytochrome P450, CYP; aldo-keto reductase, AKR; carbonyl reductase, CBR; UDP-glucuronosyltransferase, UGT; cysteine, cys; 6-methylcysteinylandrosta-1,4-diene-3,17-dione, EXE-cys; 6-methylcysteinylandrosta-1,4-diene-17b-hydroxy-3-one, DHE-cys; glutathione, GSH; time dependent inhibition, TDI; ultra performance liquid chromatography-mass spectrometry, UPLC/MS.

Molecular Pharmacology Fast Forward. Published on August 11, 2022 as DOI: 10.1124/molpharm.122.000545
This article has not been copyedited and formatted. The final version may differ from this version.

Abstract

Exemestane (EXE) is an aromatase inhibitor used to treat hormone-dependent breast cancer. EXE is extensively metabolized, with unchanged EXE and its active metabolite 17-dihydroexemestane (17-DHE) accounting for 17 and 12%, respectively, of total plasma EXE *in vivo*. The major circulating EXE metabolites are the cysteine conjugates of EXE and 17-DHE, and the 17-DHE glucuronide, which together account for 70% of total plasma EXE *in vivo*. The goal of the present study was to examine the inhibition potential of major metabolites of EXE through inhibition assays using aromatase-overexpressing cells and pooled ovarian tissues. Estrone formation was used as a measure of aromatase activity and was detected and quantified using UPLC-MS. EXE-cys, 17β-DHE, and 17β-DHE-cys all exhibited inhibition of estrone formation at both 1 μM and 10 μM concentrations, with 17β-DHE and EXE-cys showing significant inhibition of estrone formation (63% each) at 10 μM. In contrast, 17β-DHE-Gluc displayed minimal inhibition (5-8%) at both concentrations. In ovarian tissue, EXE-cys and 17β-DHE showed similar patterns of inhibition, with 49% and 47% inhibition, respectively, at 10 μM. The IC_{50} value for EXE-cys (16 ± 10 μM) was similar to 17β-DHE (9.2 ± 2.7 μM) and higher than EXE (1.3 ± 0.28 μM), and all three compounds showed time-dependent inhibition with IC_{50} shifts of 13 ± 10, 5.0 ± 2.5 and 36 ± 12-fold, respectively. Given its high circulating levels in patients taking EXE, these results suggest that EXE-cys may contribute to the pharmacologic effect of EXE *in vivo*.

Molecular Pharmacology Fast Forward. Published on August 11, 2022 as DOI: 10.1124/molpharm.122.000545
This article has not been copyedited and formatted. The final version may differ from this version.

Significance Statement

The current study is the first to examine the major phase II metabolites of EXE (EXE-cys, 17β-DHE-cys, and 17β-DHE-Gluc) for inhibition potential against the target enzyme, aromatase (CYP19A1). EXE-cys was found to significantly inhibit aromatase in a time dependent manner. Given its high circulating levels in patients taking EXE, this phase II metabolite may play an important role in reducing circulating estrogen levels *in vivo.*

Molecular Pharmacology Fast Forward. Published on August 11, 2022 as DOI: 10.1124/molpharm.122.000545
This article has not been copyedited and formatted. The final version may differ from this version.

Introduction

Breast cancer continues to be the most commonly diagnosed cancer in women, with an estimated 290,000 new cases and 43,000 breast cancer related deaths expected in the United States in 2022 (Siegel et al., 2022). More than two-thirds of all diagnosed breast cancers are estrogen receptor positive (ER+), characterized by the presence of estrogen receptors which ultimately bind to estrogen to stimulate breast gland cell proliferation (Howlader et al., 1975-2013; Osborne and Schiff, 2011). A major strategy to managing tumor growth and proliferation in ER+ breast cancer patients is through anti-estrogenic therapy by blocking estrogen biosynthesis in the final step of the conversion of androgens to estrogens by inhibiting the key enzyme aromatase with aromatase inhibitors (AIs) (Untch and Thomssen, 2010; Early Breast Cancer Trialists' Collaborative, 2015; Robertson et al., 2016). This strategy is particularly effective in postmenopausal women, due to circulating estrogen levels being lower than in premenopausal women (Ramchand et al., 2019), with the addition of AIs suppressing circulating estrogens to almost undetectable levels (Campos, 2004; Kittaneh and Glück, 2011).

Exemestane (EXE) belongs to a class of steroidal aromatase inhibitors that are structurally related to the natural substrate of aromatase, androstenedione (Lombardi, 2002a; Yadav et al., 2015). Since EXE has an androstenedione-like structure, it interacts with the substrate binding site of aromatase, forming a reactive intermediate that covalently binds to the enzyme and causes time-dependent (irreversible) inhibition (Lombardi, 2002a). EXE has shown superior clinical efficacy with fewer life-threatening

Molecular Pharmacology Fast Forward. Published on August 11, 2022 as DOI: 10.1124/molpharm.122.000545
This article has not been copyedited and formatted. The final version may differ from this version.

side effects such as endometrial cancers and thromboembolic complications as compared to the commonly used SERM, tamoxifen (Coombes et al., 2007; Goss et al., 2011). In addition, results from the international Mammary Prevention 3 trial (MAP.3) show that EXE reduced the risk of breast cancer by 65% in postmenopausal women who were at high risk for developing breast cancer based on their Gail risk score (Goss et al., 2011). Recently, updated clinical practice guidelines suggest that EXE be prescribed as an extended therapy (up to ten years) for postmenopausal women who have been diagnosed with lymph node positive ER+ breast cancer (Burstein et al., 2019; Wazir et al., 2019).

Despite its effectiveness at reducing circulating estrogen levels (85-95% at a relatively low dose of 25 mg), EXE has a low absolute bioavailability of 5% due to extensive first pass metabolism (Singh et al., 2009; Kittaneh and Glück, 2011). In phase I of its metabolic pathway, EXE is reduced to the active metabolite, 17β-dihydroexemestane (17β-DHE), by hepatic cytosolic reductases (AKR1C's 1-4), cytochrome P450s (1A2, 2C8, 2C9, 2C19, 2D6, 3A4 and 3A5) and carbonyl reductase (Kamdem et al., 2011; Platt et al., 2016; Peterson et al., 2017c). Further metabolism of exemestane and 17β-DHE proceeds through the phase II pathways of glutathionylation and glucuronidation. Glutathionylation begins with the conjugation of the tripeptide glutathione (GSH) to EXE or 17β-DHE primarily via glutathione-S-transferase A1 (Teslenko et al., 2021). Subsequent stepwise removal of the glutamine via gamma-glutamyl transferase (GGT) enzymes and the glycine via dipeptidases results in a stable cysteine conjugate (Hinchman and Ballatori, 1994; Hayes et al., 2005; Luo et al., 2018; Teslenko et al., 2021). In the glucuronidation pathway, 17β-DHE is conjugated with a

Molecular Pharmacology Fast Forward. Published on August 11, 2022 as DOI: 10.1124/molpharm.122.000545
This article has not been copyedited and formatted. The final version may differ from this version.

glucuronic acid moiety via the UDP-glucuronosyltransferase (UGT) 2B17 enzyme to form 17β-DHE-glucuronide [17β-DHE-Gluc; (Sun et al., 2010; Luo et al., 2017)].

Cysteine conjugates of EXE and 17β-DHE comprise the major metabolites in the plasma (combined = 35% of total EXE) and urine (combined = 77% of total EXE) of postmenopausal women diagnosed with ER+ breast cancer and taking EXE as a monotherapy for at least 28 days (Luo et al., 2018). In the same patient population, 17β-DHE-Gluc comprised 35% of the total EXE metabolites in plasma and 26% in urine (Luo et al., 2018). This compared to only 17% and 12% in the plasma and 1.7% and 0.14% in the urine for EXE and 17β-DHE, respectively (Luo et al., 2018). The pharmacologic effect of EXE and 17β-DHE have been extensively studied (Peterson et al., 2017b). However, the contribution of the phase II metabolites (EXE-cys, 17β-DHE-cys, and 17β-DHE-Gluc) that comprise 71% of the total EXE metabolites in plasma have not been elucidated. The focus of the current study is to comprehensively evaluate the effects of EXE metabolites on the inhibition of the aromatase enzyme.

Molecular Pharmacology Fast Forward. Published on August 11, 2022 as DOI: 10.1124/molpharm.122.000545
This article has not been copyedited and formatted. The final version may differ from this version.

Materials and Methods

Chemicals and materials

Sigma-Aldrich (St Louis, MO) supplied 4-andostene-3,17-dione, estrone and estrone-2,3,4-$^{13}C_3$. Corning (Bedford, MA) provided the NADPH regeneration system (1.3 mM NADP, 3.3 mM 6-phosphate, and 0.4 U/ml glucose 6-phosphate dehydrogenase) and dimethyl sulfoxide (DMSO). The 17β-hydroxy-EXE-17-O-β-D-glucuronide (17β-DHE-Gluc) and 17β-dihydroexemestane (17β-DHE) were purchased from Toronto Research Chemicals (Toronto, ON) while EXE was purchased from Cayman Chemical Company (Ann Arbor, MI). Liquid chromatography-mass spectrometry (LC-MS) grade formic acid and methanol as well as DMEM cell culture media and geneticin were obtained from Thermo-Fisher Scientific (Waltham, MA), and LC-MS grade ammonium formate was purchased from Sigma-Aldrich. Acquity UHPLC BEH C18 columns (1.7μm 2.1 x 50 mm) were purchased from Waters (Milford, MA). Pooled human liver cytosol (HLC) was obtained from Xenotech (Kansas City, KS). Fetal bovine serum (FBS) was provided by Avantor (Radnor Township, PA) while Pierce BCA protein assay kits were purchased from Thermo-Fisher Scientific. All other chemicals and reagents were purchased from Thermo Fisher Scientific and Sigma-Aldrich.

Inhibition assays of aromatase activity

HEK293 cells with stable overexpression of the wild type aromatase enzyme [CYP19A1; (Peterson et al., 2017b)] were used for activity screening assays. The cells were grown in DMEM medium containing 350 μg/mL of geneticin and 10% FBS,

Molecular Pharmacology Fast Forward. Published on August 11, 2022 as DOI: 10.1124/molpharm.122.000545
This article has not been copyedited and formatted. The final version may differ from this version.

harvested, and an S9 fraction was prepared using previously described protocols (Peterson et al., 2017b). The total protein concentration was determined using the Pierce BCA assay. Major phase II metabolites (17β-DHE-Gluc, EXE-cys, and 17β-DHE-cys) were screened as potential inhibitors of estrone formation in the S9 fraction of the aromatase-overexpressing cells, using EXE and its phase I metabolite 17β-DHE as positive controls. 17β-DHE-Gluc, EXE and 17β-DHE were purchased commercially (described above) while EXE-cys and 17β-DHE-cys were chemically synthesized as previously described (Luo et al., 2018). The inhibition screening assays included 125 µg of S9 protein from the aromatase overexpressing cell line, 1 µM or 10 µM of inhibitor (EXE, 17β-DHE or their metabolites), 5 µM androstenedione, 100 mM potassium phosphate buffer (pH 7.4), and 3 mM of magnesium chloride, in a final volume of 50 µL. The concentration of 5 µM androstenedione was chosen since it is significantly above the known K_m of aromatase for androstenedione (Gibb and Lavoie, 1980; Sohl and Guengerich, 2010). Linear reaction conditions were tested with respect to both protein concentration and time, with 125 µg S9 protein and a 45 min incubation time both well within the linear range of estrone formation. Methanol and DMSO (the vehicle for androstenedione and EXE and its metabolites) concentrations in the final assays were 1.2% and 0.4% respectively. The NAPDH regeneration system was added to initiate the reaction, which was incubated for 45 min at 37°C. An assay without EXE, 17β-DHE or EXE metabolite was used as the reference for uninhibited (100%) enzyme activity. Negative controls included, (1) an incubation with S9 fraction from the parent HEK293 cell line without the overexpressed aromatase enzyme, and (2) an incubation with no NADPH regeneration system. After incubation, reactions were quenched with 50 µL

Molecular Pharmacology Fast Forward. Published on August 11, 2022 as DOI: 10.1124/molpharm.122.000545
This article has not been copyedited and formatted. The final version may differ from this version.

cold acetonitrile spiked with 0.4 ppm of internal standard (estrone-2,3,4-$^{13}C_3$) and centrifuged at 4°C for 15 min at 13,200 g. Supernatants were transferred to a glass vial for analysis by UPLC-MS. Estrone formation (in ppm) was quantified using a standard curve with serial dilutions of known estrone concentrations. All experiments were performed in triplicate.

Anti-aromatase activity determinations in ovarian tissue

Three normal ovarian tissue specimens were obtained from the Cooperative Human Tissue Network (CHTN). All three specimens were from Caucasian female donors (30-40 y) and were flash frozen within two hours of removal. Each frozen tissue (250 mg) was placed in a 2 mL tube with 750 µL of homogenizing buffer (25 mM Tris Base, 138 mM NaCl, 2.7 mM KCl, pH 7.4) and a 5 mm metal bead. Tissues were homogenized with a TissueLyzer for 2 min at 20 Hz, followed by five freeze/thaw cycles (frozen in liquid nitrogen followed by thawing in a 37°C water bath). Cell homogenate was further processed on ice in a Dounce homogenizer for 30 strokes. An S9 fraction was prepared by collecting supernatant after centrifugation of the cell homogenate at 9,000 g for 30 min at 4°C. Total protein content in the S9 fraction was analyzed with the Pierce BCA kit. A pooled (n=3) ovarian S9 fraction was prepared by combining aliquot containing 2 mg protein of each ovarian S9 fraction, and inhibition screening assays were performed with 1 µM and 10 µM EXE, 17β-DHE, or EXE-cys as described above, using a total of 300 µg of pooled ovarian S9 protein in each assay.

UPLC-MS methods for estrone detection.

Molecular Pharmacology Fast Forward. Published on August 11, 2022 as DOI: 10.1124/molpharm.122.000545
This article has not been copyedited and formatted. The final version may differ from this version.

The method for estrone detection was optimized from a previously published study (Peterson et al., 2017b). Samples (3 µL) were injected onto an Acquity UPLC BEH C18 column (1.7µm 2.1 x 50 mm) and analyzed using a XEVO G2-S QToF mass spectrometer coupled to an Acquity UPLC (Waters). The total elution gradient time was 6.5 min under the following conditions: 0.2 - 2.5 min at 43%: 57% of mobile phase A (0.1% formic acid): mobile phase B (100% methanol); a linear gradient to 100% B from 2.5 – 4.0 min; and re-equilibrium with 57% B from 4.0 - 6.5 min. The flow rate was set at 0.4 mL/min and the column temperature at 35°C, while the sample temperature was kept at 10°C. Estrone was detected with the XEVO G2-S QToF operating in the MS/MS mode, with an ESI probe operating in positive-ion mode with a capillary voltage of 0.6 kV. Nitrogen was used for both the cone and desolvation gases, with flow rates of 50 and 800 L/h, respectively. The collision energy was tuned at 20V and the cone voltage at 20V for both estrone and estrone-2,3,4-$^{13}C_3$ detection. The following mass transitions were used for metabolite detection: androstenedione, m/z 287.20→287.20; estrone, m/z 271.17→133.07; and estrone-2,3,4-$^{13}C_3$, m/z 273.17→136.08. Androstenedione was monitored to make sure that it was added to all incubations and, more importantly, to make sure that it was observed at a different retention time than estrone, assuring that any measured estrone peaks were not potentially contaminated by signal interference from the androstenedione peak in our LC-MS.

IC_{50} and IC_{50} shift determinations for aromatase activity inhibition

IC_{50} values were determined for EXE-cys in the S9 fraction of the HEK293 aromatase-overexpressing cell line. Multiple concentrations of EXE-cys ranging from

Molecular Pharmacology Fast Forward. Published on August 11, 2022 as DOI: 10.1124/molpharm.122.000545
This article has not been copyedited and formatted. The final version may differ from this version.

0.01 to 100 μM were analyzed in incubations containing androstenedione, as described above. EXE and 17β-DHE IC_{50} values were also determined as positive controls and validation of the assay system, using EXE in concentrations ranging from 0.01 to 30 μM and 17β-DHE in concentrations ranging from 0.01 to 100 μM.

To determine if the inhibition occurred in a time-dependent manner, an IC_{50} shift assay was performed for all three compounds (EXE, 17β-DHE, and EXE-cys). S9 protein from the aromatase overexpressing cell line was pre-incubated with NADPH and inhibitor (0.01 to 100 μM for 17β-DHE and EXE-cys, and 30 to 0.01 μM for EXE) for 30 min at 37°C. Androstenedione (5 μM) was then added and the reaction was incubated for 45 min at 37°C. IC_{50} values were determined for incubations that contained the 30 min pre-incubation step, as well as for incubations that contained no pre-incubation step. The ratio between the IC_{50} values with a 30 min pre-incubation step and those with no pre-incubation step was calculated and presented as the IC_{50} shift. Per FDA guidelines, if the ratio is greater than 1.5, the inhibition is considered time-dependent. All IC_{50} assays were performed in triplicate.

Data Analysis

Estrone formation was quantified in ppm using TargetLynx software (Waters). Values were exported and presented as % relative activity = (estrone formation with EXE or EXE metabolite/ uninhibited estrone formation) × 100. IC_{50} values were calculated using a three parameter IC_{50} model using GraphPad Prism 7.04 software (GraphPad Software Inc., San Diego, CA) by plotting % relative activity vs. log concentration of inhibitor. The IC_{50} values were calculated in μM for each of the

Molecular Pharmacology Fast Forward. Published on August 11, 2022 as DOI: 10.1124/molpharm.122.000545
This article has not been copyedited and formatted. The final version may differ from this version.

triplicate experiments and then averaged to give a mean IC_{50}. cLogP values were obtained using ChemDraw software.

Molecular Pharmacology Fast Forward. Published on August 11, 2022 as DOI: 10.1124/molpharm.122.000545
This article has not been copyedited and formatted. The final version may differ from this version.

Results

The three major phase II metabolites of EXE (EXE-cys, 17β-DHE-cys, and 17β-DHE-Gluc) were assayed for potential inhibition of estrone formation in a HEK293 cell line overexpressing the aromatase enzyme (Peterson et al., 2017a). Parent drug, EXE, and its active phase I metabolite, 17β-DHE, were also assayed as known inhibitors of aromatase activity. Screening results (Figure 1) showed that at 1 μM final concentration, EXE was the most potent inhibitor of estrone formation, resulting in a 51% decrease in aromatase activity (49% relative activity) as compared to incubations without inhibitor (i.e., EXE or its metabolites). At 1 μM, EXE-cys, 17β-DHE, and 17β-DHE-cys exhibited similar levels of inhibition of estrone formation (28, 28, and 22%, respectively) but at levels lower than that observed for EXE. 1 μM 17β-DHE-Gluc exhibited minimal inhibition of estrone activity (< 5%). At a 10 μM final concentration, EXE, 17β-DHE, and EXE-cys each exhibited a decrease in estrone formation as compared to incubations without inhibitor (87%, 63%, and 63%, respectively). In comparison, 10 μM 17β-DHE-cys exhibited only a 35% decrease in estrone formation while 17β-DHE-Gluc again exhibited minimal inhibition of estrone formation (i.e., < 10%).

According to the human protein atlas [http://www.proteinatlas.org; queried on January 10th, 2022; (Uhlén et al., 2015)], ovaries have one of the highest levels of expression of the aromatase enzyme. Utilizing the S9 fraction from pooled ovarian tissues, anti-aromatase screening assays utilizing EXE, 17β-DHE, and EXE-cys as potential inhibitors showed similar inhibition patterns to those observed in the aromatase cell line (Figure 2). At 1 μM and 10 μM, EXE inhibited estrone formation by

Molecular Pharmacology Fast Forward. Published on August 11, 2022 as DOI: 10.1124/molpharm.122.000545
This article has not been copyedited and formatted. The final version may differ from this version.

46 and 78%, respectively (54 and 22% relative activity) in pooled ovarian S9. Similarly, 17β-DHE and EXE-cys inhibited estrone formation in ovarian tissue S9 fractions by 21 and 29%, respectively, at 1 μM, and 49 and 47%, respectively, at 10 μM.

Based on the screening results, IC_{50} values were determined for EXE and its metabolites that exhibited ≥50% inhibition (≤ 50% relative activity) of aromatase activity in S9 fractions of aromatase-overexpressing cells in the screening assays (EXE, 17β-DHE and EXE-cys; see Table 1). The major phase II metabolite, EXE-cys, exhibited an IC_{50} value of 16 ± 10 μM, which is approximately 12-fold higher than EXE (1.3 ± 0.28 μM), but was < 1.8-fold higher than the active phase I metabolite 17β-DHE (9.2 ± 2.7 μM). The previously reported IC_{50} values for EXE and 17β-DHE [0.92 ± 0.17 μM and 4.3 ± 0.56 μM, respectively; (Peterson et al., 2017b)] are similar to the values reported in the present study. Representative IC_{50} curves of all three compounds are shown in Figure 3.

All three compounds (EXE, 17β-DHE and EXE-cys) were further evaluated for time-dependent inhibition (TDI) in an IC_{50} shift assay. An IC_{50} shift of greater than 1.5 fold is indicative of TDI (Berry and Zhao, 2008). In the present study, EXE, a known time-dependent irreversible inhibitor of aromatase (Giudici et al., 1988; Zilembo et al., 1995; Lombardi, 2002b) exhibited an IC_{50} shift of 36 ± 12, well above the suggested 1.5-fold cut-off (Table 1). The major metabolites, 17β-DHE and EXE-cys exhibited IC_{50} shifts of 5.0 ± 2.5 and 13 ± 10, respectively, indicating that these inhibitors also act in a time-dependent manner (Table 1). Representative curves for the IC_{50} shift assays are shown in Figure 4.

Molecular Pharmacology Fast Forward. Published on August 11, 2022 as DOI: 10.1124/molpharm.122.000545
This article has not been copyedited and formatted. The final version may differ from this version.

Discussion

The present study is the first to comprehensively examine the major metabolites of EXE (17β-DHE, EXE-cys, 17β-DHE-cys and 17β-DHE-Gluc) for inhibition potential of the aromatase enzyme, a key target for the treatment and prevention of ER+ breast cancer. Previous studies have focused mainly on the inhibition kinetics of the parent drug, EXE, and its phase I metabolite, 17β-DHE (Buzzetti et al., 1993; Hong et al., 2007; Peterson et al., 2017a). However, the phase II metabolites (EXE-cys, 17β-DHE-cys and 17β-DHE-Gluc) combine for a total of 71% of total EXE constituents (i.e., EXE plus its metabolites) observed in the plasma of patients taking EXE as compared to 29% for the parent EXE and its phase I active metabolite, 17β-DHE (Luo et al., 2018). According to FDA guidelines for the safety testing of drug metabolites, any metabolite that is present in the plasma at greater than 10% at steady state should be further tested for the pharmacologic activity at the therapeutic target receptor or enzyme (Schadt et al., 2018). The three phase II metabolites EXE-cys, 17β-DHE-cys and 17β-DHE-Gluc are present in the plasma at 23%, 12% and 36%, respectively, warranting a comprehensive aromatase inhibition study of these metabolites.

EXE-cys, a phase II metabolite, was shown to inhibit estrogen formation by 63% at 10 μM, which was similar to the level of inhibition observed for the phase I metabolite, 17-DHE. The remaining major phase II metabolites did not reach inhibition levels of greater than 50% at 10 μM concentrations. By comparison, the level of estrogen formation inhibition observed for the parent drug EXE at this concentration was 1.4-fold higher than EXE-cys or 17β-DHE, and 2.5- and 11-fold higher than DHE-cys and 17β-DHE-Gluc, respectively. This pattern was similar to that observed in S9 fractions of

Molecular Pharmacology Fast Forward. Published on August 11, 2022 as DOI: 10.1124/molpharm.122.000545
This article has not been copyedited and formatted. The final version may differ from this version.

ovarian tissue, where EXE-cys inhibited estrone formation to a similar extent as 17β-DHE, with both metabolites approaching 50% inhibition at 10 μM. Inhibition of estrone formation in ovary S9 fractions by the parent drug, EXE, was also similar to that observed in the aromatase overexpressing cell line and was 1.6-fold higher than the inhibition observed with EXE-cys. While the calculated IC_{50} values for EXE-cys were 12-fold higher than the parent EXE, it was only marginally higher than that observed for 17β-DHE (1.77-fold). Together, these data suggest that EXE-cys exhibits significant anti-aromatase activity.

The mean circulating levels of EXE-cys in the plasma of patients with ER+ breast cancer taking EXE (22 nM) is approximately 9-fold higher than 17β-DHE and 1.6-fold higher than the parent EXE [14 nM; (Luo et al., 2018)]. While *in vitro* and *in vivo* values cannot be directly compared, the ratio of the steady state plasma concentrations (C_{ss}) of 17β-DHE, EXE and EXE-cys quantified in our previous studies (Luo et al., 2018) vs. the *in vitro* IC_{50} values calculated in the present studies (i.e., C_{ss}/IC_{50}; see Table 2) indicates that EXE-cys is approximately 7-fold lower than EXE but nearly 5-fold higher than that observed for 17β-DHE. While the Css/ IC_{50} ratio does not take into the account the unbound in vivo concentration, the cLogP value observed for EXE-cys (0.31) is ~10-fold lower than that observed for EXE or 17β-DHE, which suggests that the cysteine conjugate is less lipophilic than either the parent drug or 17β-DHE and that the unbound fraction of EXE-cys is likely higher than EXE or 17β-DHE (Ghafourian and Amin, 2013). Therefore, our *in vitro* study suggests that EXE-cys may possess a similar *in vitro* inhibitory potency as compared to EXE, further supporting an important role for EXE-cys in the overall inhibition of aromatase by EXE. Experiments designed to examine the free

Molecular Pharmacology Fast Forward. Published on August 11, 2022 as DOI: 10.1124/molpharm.122.000545
This article has not been copyedited and formatted. The final version may differ from this version.

fraction of EXE versus its major metabolites will be required to establish more definitively their individual contribution to overall EXE clinical efficacy.

Because EXE is a known time-dependent inhibitor, both EXE-cys and 17β-DHE were screened for TDI (Lombardi, 2002b). The IC_{50} shift assays show a 13- and 5-fold decrease in the IC_{50} for EXE-cys and 17β-DHE, respectively, which far exceeds the FDA's 1.5-fold threshold for a TDI, confirming that both EXE-cys and 17β-DHE also act as time-dependent inhibitors of aromatase (Berry and Zhao, 2008). These results suggest that EXE-cys is a phase II metabolite that contributes to the inhibitory pharmacologic effect on the target aromatase enzyme through a similar mechanism as the parent drug, EXE.

The mechanism of action for the parent EXE against aromatase is suicide inhibition. EXE resembles hormonal substrates of aromatase like androstenedione in structure, with a key difference of an additional 1,2 double bond that prevents full aromatization by covalent bond formation with the enzyme (Lombardi, 2002b). All three phase II metabolites, EXE-cys, 17β-DHE-cys and 17β-DHE-Gluc, have 1,2 double bonds that are essential for the inactivation of aromatase. An explanation for why enzyme inhibition was observed for cysteine conjugates but not the glucuronide conjugate may be conjugate location on the steroid ring of the EXE molecule. Previous studies have shown that C-6 substitutions on the substrate androstenedione don't typically interfere with the binding site of aromatase but protrude outside the aromatase cavity, while the C-17 position is important for hydrogen bond formation in the hydrophobic binding pocket of aromatase (Ghosh et al., 2012; Yadav et al., 2015). This is consistent with cysteine and glucuronide conjugate structures, with the cysteine

Molecular Pharmacology Fast Forward. Published on August 11, 2022 as DOI: 10.1124/molpharm.122.000545
This article has not been copyedited and formatted. The final version may differ from this version.

conjugates of EXE and 17β-DHE being located on the C-6 position, while the glucuronide conjugate is located on the C-17 position (Luo et al., 2018).

The EXE-cys metabolite is formed via conjugation of EXE with the tripeptide glutathione (GSH; γ-glu-cys-gly), catalyzed mainly by the GSTA1 enzyme, with subsequent removal of the glutamyl and glycyl groups by γ-glutamyl transferase and dipeptidases (Teslenko et al., 2021). Phase II biotransformation reactions are generally detoxifying steps in the metabolism of drugs, which make most drugs more soluble and yield pharmacologically inactive metabolites (Jancova et al., 2010). However, in some cases, conjugated products may be pharmacologically active (Obach, 2013). One example of biotransformation that leads to pharmacologically active phase II metabolites is the glucuronidation of morphine to morphine-6-glucuronide (M6G), a metabolite with a similar affinity to the target mu-opioid receptor (MOR) and results in similar analgesic effects (Mulder, 1992; Kilpatrick and Smith, 2005). Interestingly, M6G has a better safety profile then its parent drug, morphine (Mulder, 1992). In clinical studies, healthy volunteers who received M6G through IV had fewer side effects such as nausea and vomiting compared to volunteers who received morphine (Romberg et al., 2004), and M6G was found to be 19-50 times less likely to cause respiratory depression (Romberg et al., 2003).

However, not all active metabolites lead to improved efficacy with fewer severe adverse events. Reactive metabolites are a major concern in drug discovery and development, as well as in the clinic. Most commonly, these metabolites contain electrophilic moieties that can form covalent bonds with non-specific cellular proteins, causing idiosyncratic drug induced liver injury (Dahal et al., 2013; Gómez-Lechón et al.,

Molecular Pharmacology Fast Forward. Published on August 11, 2022 as DOI: 10.1124/molpharm.122.000545
This article has not been copyedited and formatted. The final version may differ from this version.

2016). The marker for a parent drug or reactive metabolite's potential to form non-specific covalent bonds is its ability to form conjugates with GSH or cysteine, since electrophiles are trapped by the thiol residues of GSH or L-cysteine (Gómez-Lechón et al., 2016). Acetaminophen (APAP) hepatotoxicity is one of the most well-known examples, in which the reactive metabolite N-acetyl-p-benzoquinone imine (NAPQ) forms the glutathione conjugate APAP-GSH. When APAP is taken at more than 4 g/day, the excess of NAPQ leads to the depletion of GSH stores. NAPQ starts forming protein adducts through non-specific binding with the cysteine groups on the mitochondrial proteins, leading to mitochondrial oxidative stress and programmed necrosis (Albano et al., 1985; Mazaleuskaya et al., 2015; Ramachandran and Jaeschke, 2018). In contrast, despite the presence of cysteine conjugates as two of its major phase II metabolites, EXE has a low covalent binding burden (under 10 mg/day), meaning this drug has low non-specific binding *in vivo* (Dahal et al., 2013). In addition, EXE is well tolerated, with mild to moderate adverse events and few hepatotoxicity events (Bao et al., 2010; Goss et al., 2011). However, EXE is taken as an adjuvant therapy in combination with chemotherapy and as a chronic treatment [up to 10 years for the prevention of breast cancer recurrence; (Burstein et al., 2019; Wazir et al., 2019)]. Long term EXE treatment and chemotherapy have been shown to induce GST expression and can lead to GSH depletion and potential toxicities or adverse events that were not previously elucidated (Townsend and Tew, 2003; Pljesa-Ercegovac et al., 2018). Interestingly, the discovery of cysteine conjugates as the major metabolite of EXE occurred in patients undergoing chronic dosing regiments (Luo et al., 2018). Earlier studies with acute dosing did not identify cysteine conjugates, suggesting a possibility for metabolite accumulation and

Molecular Pharmacology Fast Forward. Published on August 11, 2022 as DOI: 10.1124/molpharm.122.000545
This article has not been copyedited and formatted. The final version may differ from this version.

the potential for significant therapeutic or adverse effects and drug-drug interactions that have not yet been elucidated (Pfizer, 2018).

The present study suggests that the biotransformation of EXE to EXE-cys results in an active metabolite capable of TDI of the target aromatase enzyme. Since EXE is extensively metabolized by first pass metabolism, the EXE-cys metabolite may play an important role in contributing to the observed 95% decrease in the circulating levels of estrogen *in vivo* in patients taking EXE (Singh et al., 2009; Kittaneh and Glück, 2011). Further studies examining the off-target effects of EXE-cys, the potential for drug-drug interactions with major chemotherapeutic agents prescribed in combination with EXE, and the contribution of EXE-cys to overall patient response to EXE will be important to more fully understand EXE's mechanism of action and drug efficacy.

Molecular Pharmacology Fast Forward. Published on August 11, 2022 as DOI: 10.1124/molpharm.122.000545
This article has not been copyedited and formatted. The final version may differ from this version.

Acknowledgements

The authors would like to thank Shaman Luo and Bhagwat Prasad for their helpful insight and contributions to the study.

Authorship contributions

Participated in research design: Teslenko and Lazarus.

Conducted experiments: Teslenko

Contributed new reagents or analytic tools:

Performed data analysis: Teslenko

Wrote or contributed to the writing of the manuscript: Teslenko, Watson, Chen, and Lazarus.

Molecular Pharmacology Fast Forward. Published on August 11, 2022 as DOI: 10.1124/molpharm.122.000545
This article has not been copyedited and formatted. The final version may differ from this version.

References

Albano E, Rundgren M, Harvison PJ, Nelson SD, and Moldéus P (1985) Mechanisms of N-acetyl-p-benzoquinone imine cytotoxicity. *Molecular Pharmacology* **28:**306-311.

Bao T, Fetting J, Mumford L, Zorzi J, Shahverdi K, Jeter S, Herlong F, Stearns V, and Lee L (2010) Severe prolonged cholestatic hepatitis caused by exemestane. *Breast cancer research and treatment* **121:**789-791.

Berry LM and Zhao Z (2008) An examination of IC50 and IC50-shift experiments in assessing time-dependent inhibition of CYP3A4, CYP2D6 and CYP2C9 in human liver microsomes. *Drug Metab Lett* **2:**51-59.

Burstein HJ, Lacchetti C, Anderson H, Buchholz TA, Davidson NE, Gelmon KA, Giordano SH, Hudis CA, Solky AJ, Stearns V, Winer EP, and Griggs JJ (2019) Adjuvant Endocrine Therapy for Women With Hormone Receptor-Positive Breast Cancer: ASCO Clinical Practice Guideline Focused Update. *J Clin Oncol* **37:**423-438.

Buzzetti F, Di Salle E, Longo A, and Briatico G (1993) Synthesis and aromatase inhibition by potential metabolites of exemestane (6-methylenandrosta-1,4-diene-3,17-dione). *Steroids* **58:**527-532.

Campos SM (2004) Aromatase Inhibitors for Breast Cancer in Postmenopausal Women. *The Oncologist* **9:**126-136.

Coombes RC, Kilburn LS, Snowdon CF, Paridaens R, Coleman RE, Jones SE, Jassem J, Van de Velde CJ, Delozier T, Alvarez I, Del Mastro L, Ortmann O, Diedrich K, Coates AS, Bajetta E, Holmberg SB, Dodwell D, Mickiewicz E, Andersen J, Lonning PE, Cocconi G, Forbes J, Castiglione M, Stuart N, Stewart A, Fallowfield LJ, Bertelli G, Hall E, Bogle RG, Carpentieri M, Colajori E, Subar M, Ireland E, Bliss JM, and Intergroup Exemestane S (2007) Survival and safety of exemestane versus tamoxifen after 2-3 years' tamoxifen treatment (Intergroup Exemestane Study): a randomised controlled trial. *Lancet* **369:**559-570.

Dahal UP, Obach RS, and Gilbert AM (2013) Benchmarking in Vitro Covalent Binding Burden As a Tool To Assess Potential Toxicity Caused by Nonspecific Covalent Binding of Covalent Drugs. *Chemical Research in Toxicology* **26:**1739-1745.

Early Breast Cancer Trialists' Collaborative G (2015) Aromatase inhibitors versus tamoxifen in early breast cancer: patient-level meta-analysis of the randomised trials. *Lancet* **386:**1341-1352.

Ghafourian T and Amin Z (2013) QSAR models for the prediction of plasma protein binding. *BioImpacts : BI* **3:**21-27.

Ghosh D, Lo J, Morton D, Valette D, Xi J, Griswold J, Hubbell S, Egbuta C, Jiang W, An J, and Davies HML (2012) Novel Aromatase Inhibitors by Structure-Guided Design. *Journal of Medicinal Chemistry* **55:**8464-8476.

Gibb W and Lavoie JC (1980) Substrate specificity of the placental microsomal aromatase. *Steroids* **36:**507-519.

Giudici D, Ornati G, Briatico G, Buzzetti F, Lombardi P, and di Salle E (1988) 6-Methylenandrosta-1,4-diene-3,17-dione (FCE 24304): a new irreversible aromatase inhibitor. *Journal of steroid biochemistry* **30:**391-394.

Gómez-Lechón MJ, Tolosa L, and Donato MT (2016) Metabolic activation and drug-induced liver injury: in vitro approaches for the safety risk assessment of new drugs. *Journal of Applied Toxicology* **36:**752-768.

Goss PE, Ingle JN, Ales-Martinez JE, Cheung AM, Chlebowski RT, Wactawski-Wende J, McTiernan A, Robbins J, Johnson KC, Martin LW, Winquist E, Sarto GE, Garber JE, Fabian CJ, Pujol P, Maunsell E, Farmer P, Gelmon KA, Tu D, Richardson H, and Investigators NCMS (2011) Exemestane for breast-cancer prevention in postmenopausal women. *N Engl J Med* **364:**2381-2391.

Gregory BJ, Chen SM, Murphy MA, Atchley DH, and Kamdem LK (2017) Impact of the OATP1B1 c.521T>C single nucleotide polymorphism on the pharmacokinetics of exemestane in healthy post-menopausal female volunteers. *J Clin Pharm Ther* **42:**547-553.

Hayes JD, Flanagan JU, and Jowsey IR (2005) Glutathione transferases. *Annual review of pharmacology and toxicology* **45:**51-88.

Hinchman CA and Ballatori N (1994) Glutathione conjugation and conversion to mercapturic acids can occur as an intrahepatic process. *Journal of toxicology and environmental health* **41:**387-409.

Hong Y, Yu B, Sherman M, Yuan Y-C, Zhou D, and Chen S (2007) Molecular Basis for the Aromatization Reaction and Exemestane-Mediated Irreversible Inhibition of Human Aromatase. *Molecular Endocrinology* **21:**401-414.

Howlader N, Noone AM, Krapcho M, Miller D, Bishop K, Altekruse SF, Kosary CL, Yu M, Ruhl J, Tatalovich Z, Mariotto A, Lewis DR, Chen HS, Feuer EJ, and Cronin KA (1975-2013) SEER Cancer Statistics Review.

Jancova P, Anzenbacher P, and Anzenbacherova E (2010) Phase II drug metabolizing enzymes. *Biomedical papers of the Medical Faculty of the University Palacky, Olomouc, Czechoslovakia* **154:**103-116.

Kamdem LK, Flockhart DA, and Desta Z (2011) In vitro cytochrome P450-mediated metabolism of exemestane. *Drug Metab Dispos* **39:**98-105.

Kilpatrick GJ and Smith TW (2005) Morphine-6-glucuronide: actions and mechanisms. *Medicinal research reviews* **25:**521-544.

Kittaneh M and Glück S (2011) Exemestane in the adjuvant treatment of breast cancer in postmenopausal women. *Breast cancer : basic and clinical research* **5:**209-226.

Lombardi P (2002a) Exemestane, a new steroidal aromatase inhibitor of clinical relevance. *Biochim Biophys Acta* **1587:**326-337.

Lombardi P (2002b) Exemestane, a new steroidal aromatase inhibitor of clinical relevance. *Biochimica et Biophysica Acta (BBA) - Molecular Basis of Disease* **1587:**326-337.

Luo S, Chen G, Truica C, Baird CC, Leitzel K, and Lazarus P (2017) Role of the UGT2B17 deletion in exemestane pharmacogenetics. *Pharmacogenomics J*.

Luo S, Chen G, Truica CI, Baird CC, Xia Z, and Lazarus P (2018) Identification and Quantification of Novel Major Metabolites of the Steroidal Aromatase Inhibitor, Exemestane. *Drug Metab Dispos* **46:**1867-1878.

Mazaleuskaya LL, Sangkuhl K, Thorn CF, FitzGerald GA, Altman RB, and Klein TE (2015) PharmGKB summary: pathways of acetaminophen metabolism at the therapeutic versus toxic doses. *Pharmacogenetics and genomics* **25:**416-426.

Mulder GJ (1992) Pharmacological effects of drug conjugates: is morphine 6-glucuronide an exception? *Trends in pharmacological sciences* **13:**302-304.

Obach RS (2013) Pharmacologically active drug metabolites: impact on drug discovery and pharmacotherapy. *Pharmacological reviews* **65:**578-640.

Osborne CK and Schiff R (2011) Mechanisms of endocrine resistance in breast cancer. *Annu Rev Med* **62:**233-247.

Peterson A, Xia Z, Chen G, and Lazarus P (2017a) Exemestane potency is unchanged by common nonsynonymous polymorphisms in CYP19A1: results of a novel anti-aromatase activity assay examining exemestane and its derivatives. *Pharmacology research & perspectives* **5:**e00313.

Peterson A, Xia Z, Chen G, and Lazarus P (2017b) Exemestane potency is unchanged by common nonsynonymous polymorphisms in CYP19A1: results of a novel anti-aromatase activity assay examining exemestane and its derivatives. *Pharmacology research & perspectives* **5:**e00313-e00313.

Peterson A, Xia Z, Chen G, and Lazarus P (2017c) In vitro metabolism of exemestane by hepatic cytochrome P450s: impact of nonsynonymous polymorphisms on formation of the active metabolite 17beta-dihydroexemestane. *Pharmacology research & perspectives* **5:**e00314.

Pfizer (2018) Aromasin Exemestane Tablets, http://www.pfizer.com/files/products/uspi_aromasin.pdf.

Pistelli M, Mora AD, Ballatore Z, and Berardi R (2018) Aromatase inhibitors in premenopausal women with breast cancer: the state of the art and future prospects. *Curr Oncol* **25:**e168-e175.

Platt A, Xia Z, Liu Y, Chen G, and Lazarus P (2016) Impact of nonsynonymous single nucleotide polymorphisms on in-vitro metabolism of exemestane by hepatic cytosolic reductases. *Pharmacogenetics and genomics* **26:**370-380.

Pljesa-Ercegovac M, Savic-Radojevic A, Matic M, Coric V, Djukic T, Radic T, and Simic T (2018) Glutathione Transferases: Potential Targets to Overcome Chemoresistance in Solid Tumors. *International journal of molecular sciences* **19:**3785.

Ramachandran A and Jaeschke H (2018) Acetaminophen Toxicity: Novel Insights Into Mechanisms and Future Perspectives. *Gene expression* **18:**19-30.

Ramchand SK, Cheung YM, Yeo B, and Grossmann M (2019) The effects of adjuvant endocrine therapy on bone health in women with breast cancer. *J Endocrinol* **241:**R111-r124.

Robertson JFR, Bondarenko IM, Trishkina E, Dvorkin M, Panasci L, Manikhas A, Shparyk Y, Cardona-Huerta S, Cheung KL, Philco-Salas MJ, Ruiz-Borrego M, Shao Z, Noguchi S, Rowbottom J, Stuart M, Grinsted LM, Fazal M, and Ellis MJ (2016) Fulvestrant 500 mg versus anastrozole 1 mg for hormone receptor-positive advanced breast cancer (FALCON): an international, randomised, double-blind, phase 3 trial. *Lancet* **388:**2997-3005.

Romberg R, Olofsen E, Sarton E, den Hartigh J, Taschner PE, and Dahan A (2004) Pharmacokinetic-pharmacodynamic modeling of morphine-6-glucuronide-induced analgesia in healthy volunteers: absence of sex differences. *Anesthesiology* **100:**120-133.

Romberg R, Olofsen E, Sarton E, Teppema L, and Dahan A (2003) Pharmacodynamic Effect of Morphine-6-glucuronide versus Morphine on Hypoxic and Hypercapnic Breathing in Healthy Volunteers. *Anesthesiology* **99:**788-798.

Schadt S, Bister B, Chowdhury SK, Funk C, Hop CECA, Humphreys WG, Igarashi F, James AD, Kagan M, Khojasteh SC, Nedderman ANR, Prakash C, Runge F, Scheible H, Spracklin DK, Swart P, Tse S, Yuan J, and Obach RS (2018) A Decade in the MIST: Learnings from Investigations of Drug Metabolites in Drug Development under the "Metabolites in Safety Testing" Regulatory Guidance. *Drug Metabolism and Disposition* **46:**865-878.

Siegel RL, Miller KD, Fuchs HE, and Jemal A (2022) Cancer statistics, 2022. *CA Cancer J Clin* **72:**7-33.

Singh AK, Chaurasiya A, Awasthi A, Mishra G, Asati D, Khar RK, and Mukherjee R (2009) Oral bioavailability enhancement of exemestane from self-microemulsifying drug delivery system (SMEDDS). *AAPS PharmSciTech* **10:**906-916.

Sohl CD and Guengerich FP (2010) Kinetic analysis of the three-step steroid aromatase reaction of human cytochrome P450 19A1. *J Biol Chem* **285:**17734-17743.

Sun D, Chen G, Dellinger RW, Sharma AK, and Lazarus P (2010) Characterization of 17-dihydroexemestane glucuronidation: potential role of the UGT2B17 deletion in exemestane pharmacogenetics. *Pharmacogenetics and genomics* **20:**575-585.

Teslenko I, Watson CJW, Xia Z, Chen G, and Lazarus P (2021) Characterization of Cytosolic Glutathione S-Transferases Involved in the Metabolism of the Aromatase Inhibitor, Exemestane. *Drug Metab Dispos* **49:**1047-1055.

Townsend DM and Tew KD (2003) The role of glutathione-S-transferase in anti-cancer drug resistance. *Oncogene* **22:**7369-7375.

Uhlén M, Fagerberg L, Hallström BM, Lindskog C, Oksvold P, Mardinoglu A, Sivertsson Å, Kampf C, Sjöstedt E, Asplund A, Olsson I, Edlund K, Lundberg E, Navani S, Szigyarto CA-K, Odeberg J,

Djureinovic D, Takanen JO, Hober S, Alm T, Edqvist P-H, Berling H, Tegel H, Mulder J, Rockberg J, Nilsson P, Schwenk JM, Hamsten M, von Feilitzen K, Forsberg M, Persson L, Johansson F, Zwahlen M, von Heijne G, Nielsen J, and Pontén F (2015) Tissue-based map of the human proteome. *Science* **347:**1260419.

Untch M and Thomssen C (2010) Clinical practice decisions in endocrine therapy. *Cancer Invest* **28 Suppl 1:**4-13.

Wazir U, Mokbel L, Wazir A, and Mokbel K (2019) Optimizing adjuvant endocrine therapy for early ER+ breast cancer: An update for surgeons. *The American Journal of Surgery* **217:**152-155.

Yadav MR, Barmade MA, Tamboli RS, and Murumkar PR (2015) Developing steroidal aromatase inhibitors-an effective armament to win the battle against breast cancer. *European journal of medicinal chemistry* **105:**1-38.

Zilembo N, Noberasco C, Bajetta E, Martinetti A, Mariani L, Orefice S, Buzzoni R, Di Bartolomeo M, Di Leo A, Laffranchi A, and et al. (1995) Endocrinological and clinical evaluation of exemestane, a new steroidal aromatase inhibitor. *British journal of cancer* **72:**1007-1012.

Molecular Pharmacology Fast Forward. Published on August 11, 2022 as DOI: 10.1124/molpharm.122.000545
This article has not been copyedited and formatted. The final version may differ from this version.

Footnotes

These studies were made possible through the gracious support of the Public Health Service, the National Institutes of Health National Cancer Institute, U.S. Department of Health and Human Services [Grant 1R01-CA164366-01A1, to P Lazarus]. There is no conflict of interest for any of the authors for this work. Reprint requests: Philip Lazarus, Department of Pharmaceutical Sciences, College of Pharmacy and Pharmaceutical Sciences, Washington State University, Spokane, WA 99202-2131. Email: phil.lazarus@wsu.edu

Molecular Pharmacology Fast Forward. Published on August 11, 2022 as DOI: 10.1124/molpharm.122.000545
This article has not been copyedited and formatted. The final version may differ from this version.

Figure Legends

Figure 1. **Inhibition of estrone formation by major phase I and phase II metabolites of EXE in S9 fractions of HEK293 cells overexpressing recombinant aromatase enzyme.** Parent drug and metabolites were screened at 1μM and 10μM in assays containing 125 μg of S9 fraction from the aromatase overexpressing cell line. Data (± S.D.) are presented as the % relative activity = (estrone formation with metabolite)/ (uninhibited estrone formation) × 100%, with assays performed in triplicate experiments.

Figure 2. *Ex vivo* screening of EXE, 17β-DHE and EXE-cys in pooled S9 fraction from ovarian tissue. Parent drug and metabolites were screened at 1 μM and 10 μM in assays containing 300 μg of S9 fraction from ovarian tissue. Data (± S.D.) are presented as the % relative activity = (estrone formation with metabolite)/ (uninhibited estrone formation) × 100%, with assays performed in triplicate experiments.

Figure 3. Representative IC_{50} inhibition curves. Estrone formation was measured at varying concentrations of EXE, 17β-DHE, and EXE-cys. Transformed log (μM) concentrations of inhibitor are plotted against the % relative estrone formation activity.

Figure 4. Representative IC_{50} shift curves. Red lines represent the IC_{50} curves following a 30 min pre-incubation with inhibitor (i.e., activation step). Black lines represent IC_{50} curves with no pre-incubation (i.e., no activation step).

Molecular Pharmacology Fast Forward. Published on August 11, 2022 as DOI: 10.1124/molpharm.122.000545
This article has not been copyedited and formatted. The final version may differ from this version.

Table 1. IC_{50} (μM) and IC_{50} shift values of EXE and EXE metabolites using S9 fractions of HEK293 cells overexpressing recombinant aromatase enzyme.

	IC_{50} (μM) [a]	IC_{50} shift [b]
EXE-cys	16 ± 10	13 ± 10
EXE	1.3 ± 0.28	36 ± 12
17β-DHE	9.2 ± 2.7	5.0 ± 2.5

[a] IC_{50} values are expressed as the mean ± S.D. of four independent experiments.
[b] IC_{50} shift assays were performed in separate experiments than those performed for IC_{50} calculation experiments. IC_{50} shift data are the ratio between the IC_{50} with no inactivation step versus the IC_{50} plus the 30 min inactivation step. Data are expressed as the mean ± S.D. of three independent experiments.

Molecular Pharmacology Fast Forward. Published on August 11, 2022 as DOI: 10.1124/molpharm.122.000545
This article has not been copyedited and formatted. The final version may differ from this version.

Table 2. Ratios of steady state plasma concentrations observed *in vivo*[a] vs IC_{50} values observed in the present study for EXE, 17β-DHE and EXE-cys.

	C_{ss} (nM)[b]	IC_{50} (μM)	Ratio (C_{ss} / IC_{50})	cLogP
EXE	14 ± 1.7	1.3 ± 0.28	10	3.7
17β-DHE	2.5 ± 1.5	9.2 ± 2.7	0.3	3.3
EXE-cys	22 ± 2.9	16 ± 10	1.4	0.31

[a] Taken from Luo *et al.*, 2018.
[b] C_{ss}, steady state plasma concentration

Figure 1

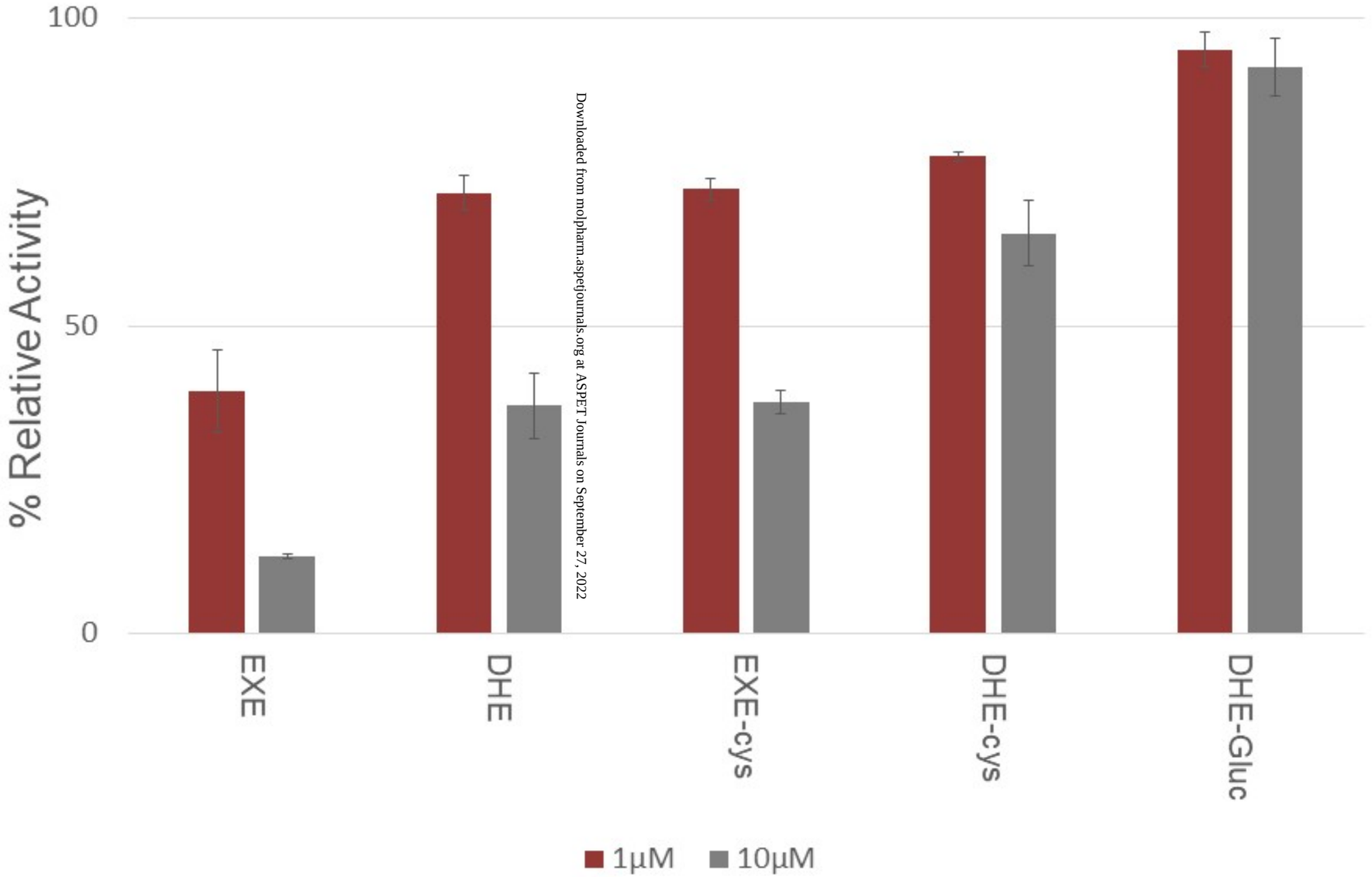

Figure 2

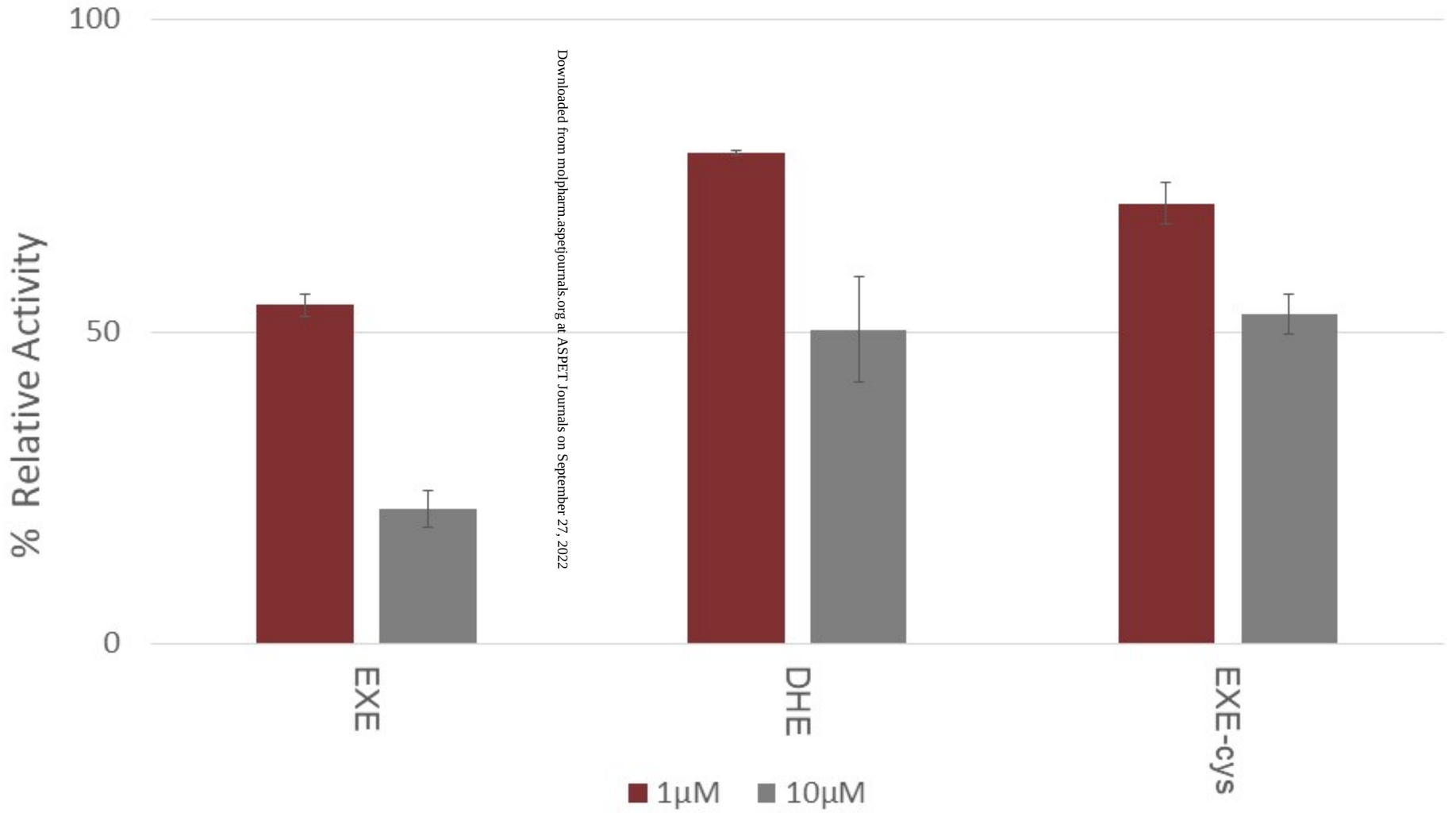

Figure 3

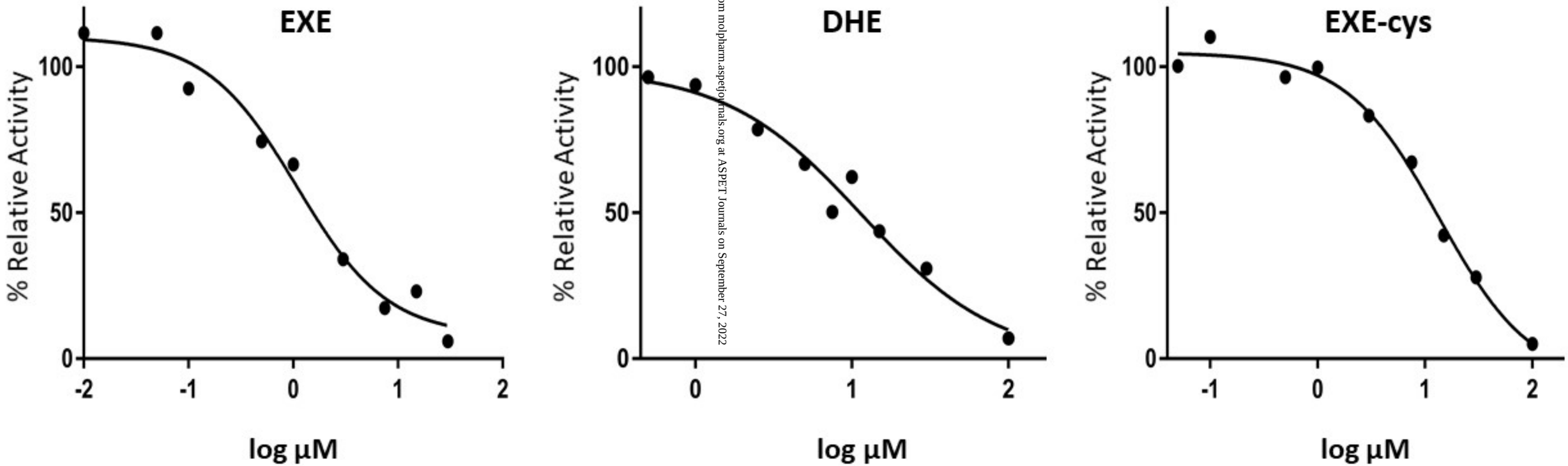

Figure 4